Inorganic Chemistry

Article

pubs.acs.org/IC

Reactivity of Diphenylpropynone Derivatives Toward Metal-Associated Amyloid-β Species

Amit S. Pithadia,[†,‡] Akiko Kochi,[†,‡] Molly T. Soper,[†] Michael W. Beck,[†] Yuzhong Liu,[†] Sanghyun Lee,[§] Alaina S. DeToma,[†] Brandon T. Ruotolo,*[,†] and Mi Hee Lim*[,†,§]

[†]Department of Chemistry and [§]Life Sciences Institute, University of Michigan, Ann Arbor, Michigan 48109, United States

Supporting Information

ABSTRACT: In Alzheimer's disease (AD), metal-associated amyloid-β (metal−Aβ) species have been suggested to be involved in neurotoxicity; however, their role in disease development is still unclear. To elucidate this aspect, chemical reagents have been developed as valuable tools for targeting metal−Aβ species, modulating the interaction between the metal and Aβ, and subsequently altering metal−Aβ reactivity. Herein, we report the design, preparation, characterization, and reactivity of two diphenylpropynone derivatives (**DPP1** and **DPP2**) composed of structural moieties for metal chelation and Aβ interaction (bifunctionality). The interactions of these compounds with metal ions and Aβ species were confirmed by UV−vis, NMR, mass spectrometry, and docking studies. The effects of these bifunctional molecules on the control of in vitro metal-free and metal-induced Aβ aggregation were investigated and monitored by gel electrophoresis and transmission electron microscopy (TEM). Both **DPP1** and **DPP2** showed reactivity toward metal−Aβ species over metal-free Aβ species to different extents. In particular, **DPP2**, which contains a dimethylamino group, exhibited greater reactivity with metal−Aβ species than **DPP1**, suggesting a structure-reactivity relationship. Overall, our studies present a new bifunctional scaffold that could be utilized to develop chemical reagents for investigating metal−Aβ species in AD.

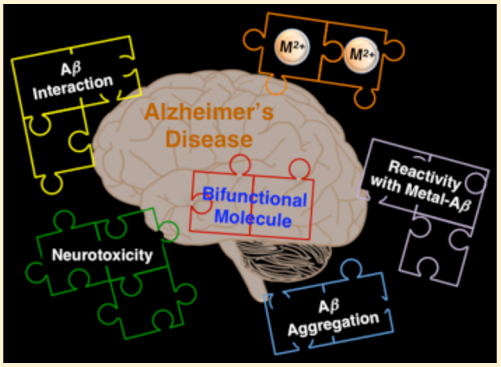

INTRODUCTION

Alzheimer's disease (AD) is a fatal neurodegenerative disease that affects more than 5 million people in the United States.[1,2] A pathological hallmark of the diseased brain is an accumulation of misfolded amyloid-β (Aβ) aggregates.[2−8] Monomeric Aβ peptides, generated from the proteolytic cleavage of the transmembrane amyloid precursor protein, can further aggregate to produce oligomers, protofibrils, and eventually fibrils. It is still not completely understood which conformation of Aβ is associated with AD neuropathogenesis; however, recent evidence has proposed that soluble oligomers might be the toxic species due to their ability to interrupt neurotransmission.[4,5,9] In addition to Aβ species, elevated concentrations of transition metals, such as Fe, Cu and Zn, have been observed within the deposits of Aβ aggregates.[2,7,8,10−15] The possible relationship between metal-associated Aβ species (metal−Aβ species) and neurotoxicity has been suggested based on observations that upon binding to Aβ, metal ions facilitate peptide aggregation as well as enhance oxidative stress caused by overproduction of reactive oxygen species;[2,4,5,7,8,12−21] however, this connection has not been clearly revealed.

To gain a better understanding of the involvement of metal−Aβ species in AD pathogenesis, recent advancements in the development of chemical reagents to specifically target metal−Aβ species and modulate their interaction and reactivity have been made.[2,7,8,21−33] Among them, rationally designed small molecules with both metal chelation and Aβ interaction properties (defined as bifunctionality) have been devised. Some of the compounds have been fashioned based on the incorporation approach (Figure 1), where a metal chelation site is directly inserted into a known Aβ imaging agent with minimal structural modifications, along with consideration of criteria for possible brain uptake.[8,21−25,27−35] These molecules have been shown to be able to control the interactions and reactivity of metal−Aβ species in vitro and/or in living cells, suggesting that the incorporation approach (Figure 1) could be considered as a promising design strategy to fashion suitable chemical reagents for uncovering the potential role of metal−Aβ species in AD development.

Herein, we report the design and preparation of a new class of bifunctional small molecules (**DPP1** and **DPP2**, Figure 1), composed of a diphenylpropynone framework, as chemical reagents for targeting and regulating metal−Aβ species, the characterization of their interactions with metal ions and Aβ species, as well as the investigation of their in vitro reactivity with metal−Aβ species. From our overall results and observations, the diphenylpropynone scaffold could be a structural feature for constructing chemical reagents for investigating metal−Aβ species. Moreover, the dimethylamino functionality in **DPP2** was observed to be an important moiety

Received: September 25, 2012
Published: November 15, 2012

   dx.doi.org/10.1021/ic302084g | *Inorg. Chem.* 2012, 51, 12959−12967

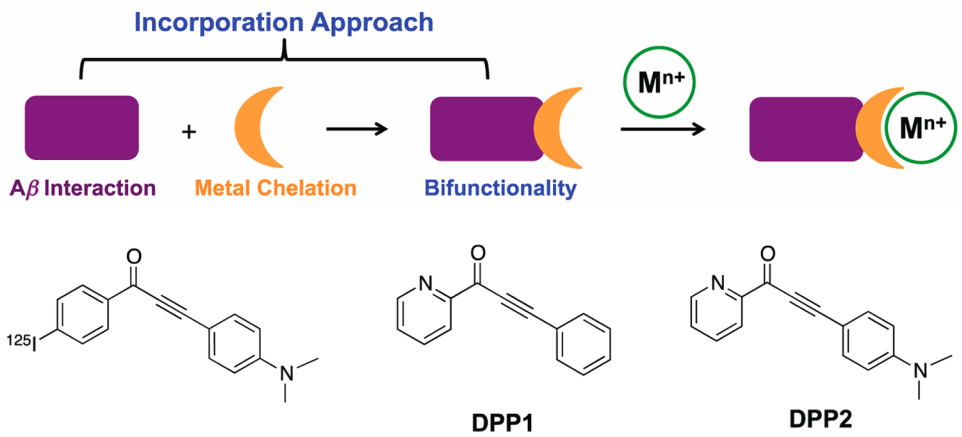

Figure 1. Incorporation approach (top) and structures of small molecules (bottom). Left to right: 3-(4-(dimethylamino)phenyl)-1-(4-iodophenyl)prop-2-yn-1-one; **DPP1** = 3-phenyl-1-(pyridin-2-yl)prop-2-yn-1-one; **DPP2** = 3-(4-(dimethylamino)phenyl)-1-(pyridin- 2-yl)prop-2-yn-1-one.

Scheme 1. Synthesis of DPP2

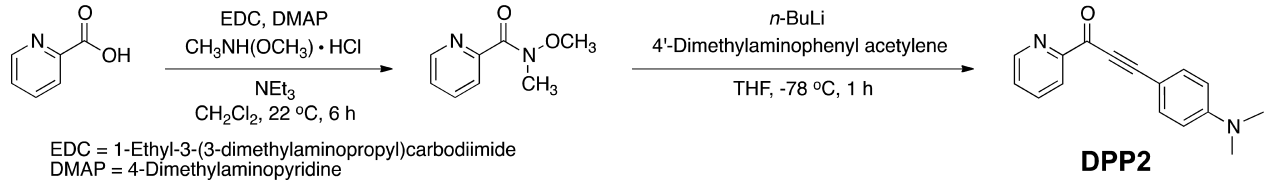

EDC = 1-Ethyl-3-(3-dimethylaminopropyl)carbodiimide
DMAP = 4-Dimethylaminopyridine

for potentially enhancing Aβ interaction of the compound, as reported previously,[29,31,36] offering noticeable reactivity with metal−Aβ species.

EXPERIMENTAL SECTION

Materials and Procedures. All reagents were purchased from commercial suppliers and used as received unless otherwise stated. The compound, 3-phenyl-1-(pyridin-2-yl)prop-2-yn-1-one (**DPP1**), was prepared following previously reported methods.[37−39] $A\beta_{1-40}$ (DAEFRHDSGYEVHHQKLVFFAEDVGSNKGAIIGLMVGGVV) was purchased from AnaSpec (Fremont, CA). An Agilent 8453 UV−visible (UV−vis) spectrophotometer was used to measure the optical spectra. Transmission electron microscopy (TEM) images were recorded with a Philips CM-100 transmission electron microscope. A SpectraMax M5 microplate reader (Molecular Devices, Sunnyvale, CA) was employed for the measurement of absorbance for 3-(4,5-dimethylthiazol-2-yl)-2,5-diphenyltetrazolium bromide (MTT) and parallel artificial membrane permeability (PAMPA) assays. Nuclear magnetic resonance (NMR) spectra of small molecules and for Zn^{2+} binding studies were obtained on a Varian 400 MHz NMR spectrometer. Mass spectrometric measurements for compounds were conducted by a Micromass LCT electrospray time-of-flight mass spectrometer. Mass spectrometric studies for investigating the interaction of **DPP1** and **DPP2** with the peptide were carried out on a Waters Synapt G2 ion-mobility mass spectrometer (Milford, MA).

Preparation of 3-(4-(Dimethylamino)phenyl)-1-(pyridin-2-yl)-prop-2-yn-1-one (DPP2). **DPP2** was synthesized by slight modifications to a previously reported procedure (Scheme 1).[39] To a solution of 4′-dimethylaminophenyl acetylene (0.42 g, 2.9 mmol) in dry tetrahydrofuran (THF, 5 mL) was added *n*-butyllithium (0.72 mL, 2.9 mmol, 2.5 M solution in hexanes) dropwise by a syringe over 5 min at −40 °C. The reaction mixture was allowed to stir at −40 °C for 10 min and then warmed to −15 °C. After 30 min, the mixture was cooled to −78 °C (dry ice/acetone) and a solution of Weinreb's amide (0.40 g, 2.4 mmol in 9 mL of dry THF) was introduced through a syringe. The reaction mixture was allowed to react at −78 °C for 10 min and then warmed to room temperature and followed by 1 h stirring. The reaction was quenched by adding saturated aqueous $NaHCO_3$ (2 mL), diluted with EtOAc (10 mL), and washed with brine (2 × 25 mL). The aqueous layer was extracted with EtOAc (2 × 15 mL), and the combined organic solutions were dried over $MgSO_4$ and filtered, followed by removal of the solvent in vacuo. The crude product was purified by silica gel chromatography (CH_2Cl_2:EtOAc = 9:1) to yield an orange product (202 mg, 0.81 mmol, 28%). ^{1}H NMR (400 MHz, $CDCl_3$)/δ (ppm): 8.77 (d, J = 4.8 Hz, 1 H), 8.14 (d, J = 7.6 Hz, 1 H), 7.82 (td, J = 7.6, 1.6 Hz, 1 H), 7.57 (d, J = 8.4 Hz, 2 H), 7.44 (m, 1 H), 6.59 (d, J = 8.4 Hz, 2 H), 2.98 (s, 6 H). ^{13}C NMR (100 MHz, $CDCl_3$)/δ (ppm): 177.6, 153.7, 151.8, 149.7, 136.8, 135.6, 126.9, 123.3, 111.4, 105.5, 100.2, 89.3, 39.9. HRMS: Calcd for $[M+H]^+$, 251.1179; found, 251.1176.

Parallel Artificial Membrane Permeability Assay Adapted for Blood-Brain Barrier (PAMPA-BBB). PAMPA-BBB experiments were carried out using the PAMPA Explorer kit (*p*ION Inc., Billerica, MA) with modification to previously reported protocols.[29,40−42] Each stock solution was diluted with pH 7.4 Prisma HT buffer (*p*ION) to a final concentration of 25 μM (1% v/v final DMSO concentration) and 200 μL were added to the wells of the donor plate (number of replicates = 12). BBB-1 lipid formulation (5 μL, *p*ION) was used to coat the polyvinylidene fluoride (PVDF, 0.45 μM) filter membrane on the acceptor plate. The acceptor plate was placed on top of the donor plate forming a sandwich and the brain sink buffer (BSB, 200 μL, *p*ION) was added to each well of the acceptor plate. The sandwich was incubated for 4 h at ambient temperature without stirring. UV−vis spectra of the solutions in the reference, acceptor, and donor plates were measured using a microplate reader. The PAMPA Explorer software v. 3.5 (*p*ION) was used to calculate the $-\log P_e$ values for the compounds. CNS± designations were assigned by comparison to compounds that were identified in previous reports.[29,40−42]

Determination of Solution Speciation for DPP1, DPP2, and the Cu^{2+}−DPP2 Complex. The pK_a values for **DPP1** and **DPP2** were determined by UV−vis variable-pH titrations as previously reported.[27,29−33,43,46] To establish the pK_a values, a solution (100 mM NaCl, 10 mM NaOH, pH 12) of **DPP1** (40 μM) or **DPP2** (20 μM) was titrated with small aliquots of HCl. At least 30 spectra were recorded in the range of pH 2−10. Similarly, a solution containing **DPP2** (20 μM) and $CuCl_2$ in a ratio of 2:1 was titrated with small additions of HCl and at least 30 spectra were recorded over the range

dx.doi.org/10.1021/ic302084g | *Inorg. Chem.* 2012, 51, 12959−12967

of pH 2−7. The acidity and stability constants were calculated by using the HypSpec program (Protonic Software, UK).[44] Speciation diagrams for **DPP1**, **DPP2**, and Cu^{2+}−**DPP2** complexes were modeled by the HySS2009 program (Protonic Software).[45]

Metal Binding Studies. The interaction of **DPP1** and **DPP2** with Cu^{2+} and Zn^{2+} was determined by UV−vis and ^{1}H NMR spectroscopy, respectively, based on previously reported procedures.[28−33,46] A solution of ligand (20 μM in EtOH) was prepared, treated with 1 to 20 equiv of $CuCl_2$, and incubated at room temperature for 2.5 h (for **DPP1**) or 5 min (for **DPP2**). The optical spectra of the resulting solutions were measured by UV−vis. The interaction of **DPP1** or **DPP2** with $ZnCl_2$ was observed by ^{1}H NMR. $ZnCl_2$ (1 equiv) was added to a solution of **DPP1** or **DPP2** (4 mM) in CD_3CN. The metal selectivity of both compounds was investigated by measuring the optical changes upon addition of 1 equiv of $CuCl_2$ to a solution of ligand (**DPP1** = 40 μM; **DPP2** = 20 μM in EtOH) pretreated with 1 or 25 equiv of a divalent metal chloride salt ($MgCl_2$, $CaCl_2$, $MnCl_2$, $FeCl_2$, $CoCl_2$, $NiCl_2$, or $ZnCl_2$). The Fe^{2+} samples were prepared anaerobically (all solutions were purged with N_2). Quantification of the metal selectivity was calculated by comparing and normalizing the absorption values of metal−ligand complexes at 360 nm (for **DPP1**) or 580 nm (for **DPP2**) to the absorption at these wavelengths before and after the addition of $CuCl_2$ (A_M/A_{Cu}). Cu^{2+} binding of **DPP2** in the presence of Aβ was examined by UV−vis. Aβ (25 μM) was treated with $CuCl_2$ (25 μM) in 20 mM HEPES (2-[4-(2-hydroxyethyl)-piperazin-1-yl]ethanesulfonic acid), pH 6.6, 150 mM NaCl for 2 min at room temperature. **DPP2** (50 μM) was added to the resulting solution, followed by 0.5−4 h incubation. For comparison, the optical spectra of **DPP2** (50 μM) were measured in the absence and presence of $CuCl_2$ (25 μM; 0.5−4 h incubation) without Aβ at pH 6.6.

*Aβ Interaction of **DPP1** and **DPP2** by Mass Spectrometry.* The interaction of **DPP1** or **DPP2** with Aβ_{1-40} was investigated by nanoelectrospray ionization-mass spectrometry (nESI-MS) that was carried out on a Synapt G2 quadrupole-ion mobility-mass spectrometry system. Samples were prepared by mixing stock solutions of **DPP1** or **DPP2** (prepared in DMSO) and Aβ_{1-40} (dissolved in 100 mM ammonium acetate, pH 6.8) to generate desired final concentrations of the peptide and the compound. Mixtures were incubated on ice or at room temperature for 2 or 4 h, respectively, and then analyzed. To produce protein complex ions, an aliquot of the sample (ca. 5 μL) was sprayed from the nESI emitter using a capillary voltage of 1.4 kV, with the source operating in positive ion mode and the sample cone operated at 50 V. To normalize nESI-MS data for nonspecific and electrospray artifact interactions that could occur at high concentrations, data were acquired for Aβ samples containing thioflavin-T (ThT), a compound known to have no affinity for soluble forms of the Aβ peptide,[47] under identical concentration conditions as our **DPP1** and **DPP2** experiments. Any ThT binding observed was assumed to be due to either nonspecific binding or the electrospray process, and subtracted from the intensities of the **DPP1** and **DPP2** interactions observed.[48] This procedure was performed over a broad range of concentrations. The mass spectra were acquired with the following settings and tuned to avoid ion activation and to preserve noncovalent protein−ligand complexes:[49] backing pressure, 7.3 mbar; IMS pressure reading, 3.09 mbar; ToF analyzer pressure, 1.14×10^{-6} mbar.

Docking Studies. Flexible ligand docking studies using AutoDock Vina[50] for **DPP1** and **DPP2** were conducted against the Aβ_{1-40} monomer from the previously determined aqueous solution NMR structure (PDB 2LFM).[51] Ten conformations were selected from 20 conformations within the PDB file (1, 3, 5, 8, 10, 12, 13, 16, 17, and 20). The MMFF94 energy minimization in ChemBio3D Ultra 11.0 was used to optimize the structures of the ligands for the docking studies. The structural files of **DPP1**, **DPP2**, and the peptide, generated by AutoDock Tools and imported into PyRx,[52] were used to run AutoDock Vina. The search space dimensions were set to contain the entire peptide. The exhaustiveness for the docking runs was set at 1024. Docked poses of the ligands were visualized with Aβ using Pymol.

Amyloid-β (Aβ) Peptide Experiments. Aβ_{1-40} was used in all Aβ experiments. Aβ_{1-40} peptide (1 mg) was dissolved with ammonium hydroxide (NH_4OH, 1% v/v, aq), aliquoted, lyophilized, and stored at −80 °C. A stock solution (ca. 200 μM) was prepared by redissolving Aβ with NH_4OH (1% v/v, aq, 10 μL) followed by dilution with ddH_2O. All Aβ solutions were prepared following previously reported procedures.[28−32] The buffered solutions (20 μM HEPES, pH 6.6 (for Cu^{2+} samples) or pH 7.4 (for metal-free and Zn^{2+} samples), 150 μM NaCl) were used for both inhibition and disaggregation studies. For the inhibition experiment, Aβ (25 μM) was first treated with a metal chloride salt ($CuCl_2$ or $ZnCl_2$, 25 μM) for 2 min followed by addition of a compound (**DPP1** or **DPP2**, 50 μM in DMSO, 1% v/v final DMSO concentration). The resulting samples were incubated at 37 °C for 4, 8, or 24 h with constant agitation. For the disaggregation experiment, Aβ and a metal chloride salt ($CuCl_2$ or $ZnCl_2$) were initially incubated at 37 °C for 24 h with steady agitation. The compound was added afterward followed by additional 4, 8, or 24 h incubation at 37 °C with constant agitation.

Native Gel Electrophoresis/Sodium Dodecyl Sulfate-Polyacrylamide Gel Electrophoresis (SDS-PAGE) with Western Blotting. The Aβ peptide experiments (as described above) were analyzed by both native gel electrophoresis and SDS-PAGE with Western blotting using an anti-Aβ antibody (6E10).[28−32,53] Each sample containing 25 μM Aβ (10 μL) was separated using either a 10−20% gradient Tris-tricine gel (Invitrogen, Grand Island, NY) or SDS gel (4% stacking gel; 10% resolving gel; nonreducing conditions). The gel was transferred to a nitrocellulose membrane and blocked overnight with bovine serum albumin (BSA, 3% w/v, Sigma, St. Louis, MO) dissolved in Tris-buffered saline (TBS, Fisher, Pittsburgh, PA) containing 0.1% Tween-20 (TBS-T, Sigma). The membrane was treated with 6E10 (1:2,000; 2% BSA in TBS-T, Covance, Princeton, NJ) for 4 h at room temperature. The membrane was probed with a horseradish peroxidase-conjugated goat anti-mouse secondary antibody (1:5000; Cayman Chemical, Ann Arbor, MI) in 2% BSA in TBS-T solution for 1 h at room temperature. The protein bands were visualized using the Thermo Scientific Supersignal West Pico Chemiluminescent Subtrate (Rockford, IL).

Transmission Electron Microscopy (TEM). Samples for TEM were prepared following a previously reported method.[28−31,33,53] Glow-discharged grids (Formar/Carbon 300-mesh, Electron Microscopy Sciences, Hatfield, PA) were treated with samples from either inhibition or disaggregation experiments (5 μL) for 2 min at room temperature. Excess sample was removed with filter paper and washed with ddH_2O five times. Each grid was stained with uranyl acetate (1% w/v, ddH_2O, 5 μL) for 1 min. Uranyl acetate was blotted off and grids were dried for 15 min at room temperature. Images of samples were taken by a Philips CM-100 transmission electron microscope (80 kV, 25,000x magnification).

Cytotoxicity (MTT Assay). The murine neuro-2a (N2a) neuroblastoma cell line was purchased from the American Type Culture Collection (ATCC, Manassas, VA). The cell line was maintained in media containing 45% Dulbecco's modified Eagle's medium (DMEM) and 50% OPTI-MEM (GIBCO, Grand Island, NY), supplemented with 5% fetal bovine serum (FBS, Sigma), 2 mM glutamine, 100 U/mL penicillin, and 100 mg/mL streptomycin (GIBCO). The cells were grown and maintained at 37 °C in a humidified atmosphere with 5% CO_2. Cell viability upon treatment of compounds was determined using a MTT assay (Sigma). N2a cells were seeded in a 96 well plate (15 000 cells in 100 μL per well) and treated with various concentrations of **DPP1** and **DPP2** (2.5−50 μM, final 1% v/v DMSO). After 24 h incubation at 37 °C, 25 μL MTT (5 mg/mL in phosphate buffered saline, PBS, pH 7.4, GIBCO) was added to each well and the plates were incubated for 4 h at 37 °C. Formazan produced by the cells was dissolved overnight at room temperature by addition of a solution (100 μL) containing *N,N*-dimethylformamide (DMF, 50% v/v, aq, pH 4.5) and sodium dodecyl sulfate (SDS, 20% w/v). A microplate reader was used to measure the absorbance (A_{600}).

RESULTS AND DISCUSSION

Design Consideration, Preparation, and Characterization of Diphenylpropynone Derivatives for Targeting and Modulating Metal−Aβ Species. The diphenylpropynone scaffold was shown to have high binding affinity (ca. 6 nM) for Aβ aggregates; thus, it has been utilized for the design of an Aβ plaque imaging probe (Figure 1).[54] Based on the incorporation approach, a nitrogen donor atom was installed into this framework to generate a metal chelation site with an oxygen donor atom from the carbonyl group, which afforded two bifunctional molecules (**DPP1** and **DPP2**, Figure 1). Furthermore, a minor structural difference between **DPP1** and **DPP2** (i.e., a dimethylamino functionality, suggested to be critical for Aβ interaction)[29,31,36] was included to understand a structure-eactivity relationship. **DPP1** was synthesized as previously established.[37−39] The new compound, **DPP2**, was prepared by slight modifications to a previously reported method (Scheme 1).[39]

To predict potential druglike and BBB penetration properties of the structural scaffolds of **DPP1** and **DPP2**, we calculated values of Lipinski's rules and logBB.[7,34,35,40,41] As shown in Table 1, the theoretical values indicate that both compounds

Table 1. Values (MW, *c*logP, HBA, HBD, PSA, logBB, and $-\log P_e$) of DPP1 and DPP2

calculation[a]	DPP1	DPP2	Lipinski's rules and others
MW	207	250	≤450
*c*log*P*	2.47	2.63	≤5.0
HBA	2	3	≤10
HBD	0	0	≤5
PSA	30.0	33.2	≤90 Å^2
logBB	0.0618	0.0390	>0.3 (readily cross the BBB)
			<−1.0 (poorly distributed in the brain)
$-\log P_e$[b]	4.2 ± 0.1	4.2 ± 0.1	
CNS± prediction[c]	CNS+	CNS+	$-\log P_e$ < 5.4 (CNS+)
			$-\log P_e$ > 5.7 (CNS−)

[a]MW, molecular weight; *c*log*P*, calculated logarithm of the octanol−water partition coefficient; HBA, hydrogen-bond acceptor atoms; HBD, hydrogen-bond donor atoms; PSA, polar surface area; logBB = −0.0148 × PSA + 0.152 × *c*log*P* + 0.130. [b]The values of $-\log P_e$ were measured by the parallel artificial membrane permeability assay (PAMPA). [c]Compounds categorized as CNS+ have the ability to permeate through the BBB and target the CNS. In the case of compounds assigned as CNS− they have poor permeability through the BBB and therefore, their bioavailability into the CNS is considered to be minimal.

are druglike and possibly BBB permeable. To verify this prediction for BBB penetration of compounds, we performed in vitro PAMPA-BBB following a previously reported procedure.[29,40−42] Permeability values ($-\log P_e$) were measured to be 4.2 (± 0.1) for both **DPP1** and **DPP2** (Table 1). On the basis of empirical classification of BBB-permeable molecules (i.e., verapamil),[29,40−42] **DPP1** and **DPP2** would also be likely to cross the BBB.

Along with BBB permeability, the solution speciation of **DPP1** and **DPP2** was determined through UV−vis variable-pH titration experiments (I = 0.10 M NaCl; room temperature; pH 2−10).[27,29−33,43,46] As summarized in Figure 2, titration results

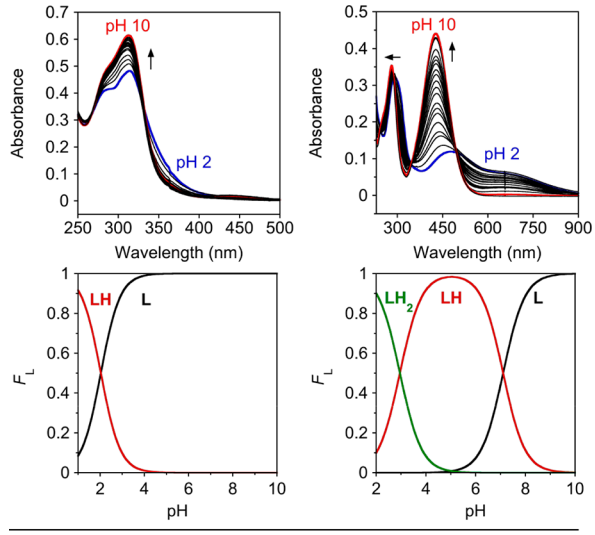

			pK_a[a] DPP1	pK_a[a] DPP2
LH_2	⇌ LH + H	(pK_{a1})	–	7.106(1)
LH	⇌ L + H	(pK_{a2})	2.035(5)	2.959(4)

Figure 2. Solution speciation studies of **DPP1** and **DPP2**. Top: UV−vis spectra of **DPP1** (40 μM, left) and **DPP2** (20 μM, right) in the range of pH 2−10. Middle: Solution speciation diagrams for **DPP1** (left) and **DPP2** (right) (F_L = fraction of compound with given protonation). Bottom: Acidity constants (pK_a) of L (L = **DPP1** or **DPP2**). Charges are omitted for clarity. [a]Error in the parentheses is shown in the last digit. Conditions: I = 0.10 M NaCl; room temperature.

indicated a single acidity constant (pK_a) for **DPP1** (pK_a = 2.035(5)) and two pK_a values for **DPP2** (pK_{a1} = 7.106(1) and pK_{a2} = 2.959(4)). These pK_a values suggest that monoprotonated, diprotonated, and neutral species exist in solution of **DPP2** depending on pH (from 2 to 10), while the monoprotonated and neutral forms of **DPP1** are present in this pH range (Figure 2). In addition, the generated solution speciation diagrams of **DPP1** and **DPP2** exhibit that their neutral forms are relatively predominant at physiologically relevant pH (i.e., 7.4) (**DPP1**, 100%; **DPP2**, ca. 65%).

Metal Binding Properties of DPP1 and DPP2. Metal binding properties of **DPP1** and **DPP2** (specifically, Cu^{2+} and Zn^{2+}) were studied by UV−vis and NMR spectroscopy. Upon the addition of $CuCl_2$ (1−20 equiv) to a solution of **DPP1** and **DPP2** in EtOH, new optical bands were observed, indicative of Cu^{2+} binding to the ligand (Figure 3a). In particular, in the presence of Cu^{2+}, **DPP2**, which has a dimethylamino group, showed a distinguishable optical shift from 407 to 525 nm. NMR was employed to investigate the interaction of **DPP1** or **DPP2** with Zn^{2+}. When 1 equiv of $ZnCl_2$ was introduced in a solution of **DPP1** or **DPP2** (in CD_3CN), noticeable downfield chemical shifts of the pyridyl protons were recorded (Figure 3b), demonstrating that Zn^{2+} binding to the ligand occurred through the pyridyl N-donor atom.[46] Overall, both UV−vis and NMR studies confirmed Cu^{2+} and Zn^{2+} binding to **DPP1** and **DPP2**.

To further identify binding stoichiometry and affinity, the solution speciation investigation of the Cu^{2+}−**DPP2** complexes was carried out through UV−vis variable-pH titration experiments (1:2 [Cu^{2+}]/[**DPP2**]; I = 0.10 M NaCl, room

dx.doi.org/10.1021/ic302084g | *Inorg. Chem.* 2012, 51, 12959−12967

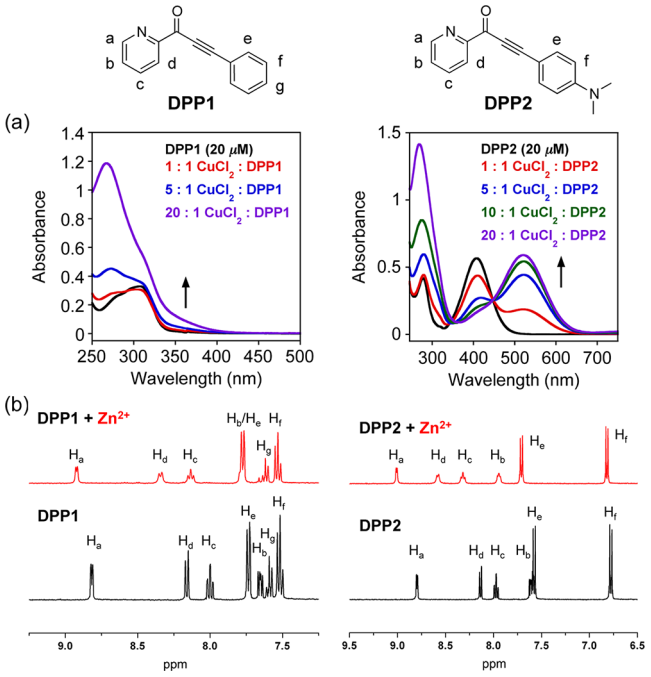

Figure 3. Cu^{2+} or Zn^{2+} binding of **DPP1** and **DPP2**. (a) UV–vis spectra of **DPP1** (left) and **DPP2** (right) with $CuCl_2$ (1–20 equiv) in EtOH at room temperature (incubation for 2.5 h (for **DPP1**) and 5 min (for **DPP2**)). (b) ^1H NMR spectra of **DPP1** (left, black) or **DPP2** (right, black) with $ZnCl_2$ (red) in CD_3CN at room temperature ([compound] = 4 mM; [$ZnCl_2$] = 4 mM).

temperature). Based on the pK_a values of **DPP2** and these titration results, stability constants for the Cu^{2+}–**DPP2** complexes were obtained (Figure 4, M + LH ⇌ M(LH) (log β_1 = 12.99(9)); M + L ⇌ ML (log β_2 = 5.85(3)); M = Cu^{2+}, L = **DPP2**). A solution speciation diagram was generated from these stability constants, suggesting that the major species at

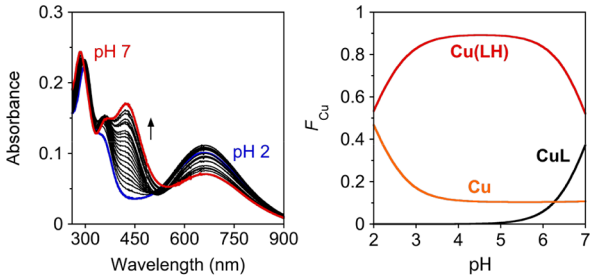

			$\log\beta^{a,b}$
Cu + LH	⇌	Cu(LH)	12.99(9)
Cu + L	⇌	CuL	5.85(3)
Cu + 2L	⇌	CuL_2	1.7(6)

Figure 4. Solution speciation investigation of the Cu^{2+}–**DPP2** complexes. Top left: UV–vis spectra (pH 2–7) for the Cu^{2+}–**DPP2** complexes ([Cu^{2+}]/[L] = 1:2; $[Cu^{2+}]_{total}$ = 10 μM; 7 h incubation with ligand (L) prior to pH titration, L = **DPP2**; room temperature). Top right: Solution speciation diagram of the Cu^{2+}–**DPP2** complexes (F_{Cu} = fraction of free Cu and Cu complexes). Bottom: Stability constants (log β) of the Cu^{2+}–**DPP2** complexes. Charges are omitted for clarity. [a]Error in the parentheses is shown in the last digit. [b]The species containing CuL_2 was introduced into the calculation model yielding a good fit to the data.

pH 7 are a mixture of Cu(LH) and CuL complexes in a ratio of 3:2. Free Cu^{2+} was shown up to pH 7, indicating pCu = 6.6 at pH 6.6 (pCu = $-\log[Cu_{unchelated}]$) (Figure 4).[27,29,31–33,43,46] The pCu value suggests the approximate dissociation constant (K_d) of Cu^{2+}–**DPP2** to be *ca.* high nanomolar. When compared to the reported K_d values of Cu^{2+}–Aβ (picomolar to nanomolar),[2,5,7,8,12,14,21] **DPP2** may interact with Cu^{2+} from soluble Cu^{2+}–Aβ species. In order to test if Cu^{2+} binding of ligand occurs in the presence of Aβ, a solution containing **DPP2** with Cu^{2+}-treated Aβ was monitored by UV–vis. The new spectral features that coincided with those of the Cu^{2+}–**DPP2** complex without Aβ were observed, suggesting an interaction of **DPP2** with Cu^{2+} in the presence of Aβ (see Figure S1 in the Supporting Information). Cu^{2+} binding of **DPP2** with Aβ occurred more slowly than that without Aβ, proposing that Aβ might interfere with metal binding to the ligand. Taken together, our spectroscopic studies present the capability of **DPP1** and **DPP2** to chelate Cu^{2+} and Zn^{2+}, as well as the potential interaction of **DPP2** with Cu^{2+} in the presence of Aβ species, which may be associated with its noticeable reactivity toward metal–Aβ species (vide infra).

The metal selectivity of **DPP1** and **DPP2** was also determined by competitive reactions with Cu^{2+} over biologically relevant divalent metal ions (Mg^{2+}, Ca^{2+}, Mn^{2+}, Fe^{2+}, Co^{2+}, Ni^{2+}, and Zn^{2+}), which was monitored by UV–vis. As depicted in Figure S2 in the Supporting Information, **DPP1** and **DPP2** displayed selectivity for Cu^{2+} over Mg^{2+}, Ca^{2+}, Mn^{2+}, and Zn^{2+}. Binding of both ligands to Co^{2+} and Ni^{2+} was also observed. Considering the lower abundance of Co^{2+} and Ni^{2+} than Cu^{2+} in biological systems,[55,56] the overall metal selectivity of **DPP1** and **DPP2** may be sufficient to be used for targeting and interacting with Cu^{2+}–Aβ species in heterogeneous biological environments like the brain.

Aβ Interaction with DPP1 and DPP2 Studied by MS and Docking Studies. The interaction of **DPP1** and **DPP2** with Aβ_{1-40} in the absence of metal ions was probed by ESI-MS, tuned to preserve noncovalent protein–ligand interactions.[49] At a low Aβ concentration (10 μM), a small signal corresponding to the interaction between **DPP2** (30 μM) and the Aβ monomer in the 3^+ charge state could be detected, whereas no interaction between **DPP1** (60 μM) and the peptide was observed under these conditions (see Figure S3 in the Supporting Information). At high concentrations of the peptide (100 μM) and compounds (600 μM), both **DPP1** and **DPP2** interacted with Aβ species to different extents (Figure 5a). Data for **DPP1** indicated that the molecule interacted broadly with Aβ monomers and oligomers in 1:1, 2:1, and 3:1 Aβ to ligand ratios. In the case of **DPP2**, a stronger preference toward larger Aβ oligomers was shown, but with similar stoichiometries as **DPP1**. The total bound intensities recorded from MS data, and those from individual oligomeric species were shown in Figure 5b and Table S1 in the Supporting Information. The intensities shown were normalized for both nonspecific interactions and artifactual complexes formed during the electrospray process using Aβ:ThT binding data as a control, and ion mobility separation was used to separate oligomers that overlapped in m/z.[6,49,57] From these data, it was clear that, at high concentrations, a higher proportion of **DPP1** was bound to Aβ species than **DPP2**, but that both could be classified as having weak Aβ affinity in solution (low mM K_d). Therefore, a weak Aβ/compound interaction was captured by MS. Normalized intensity MS data suggest that **DPP2** binding was almost exclusively driven through Aβ multimer interactions

dx.doi.org/10.1021/ic302084g | Inorg. Chem. 2012, 51, 12959–12967

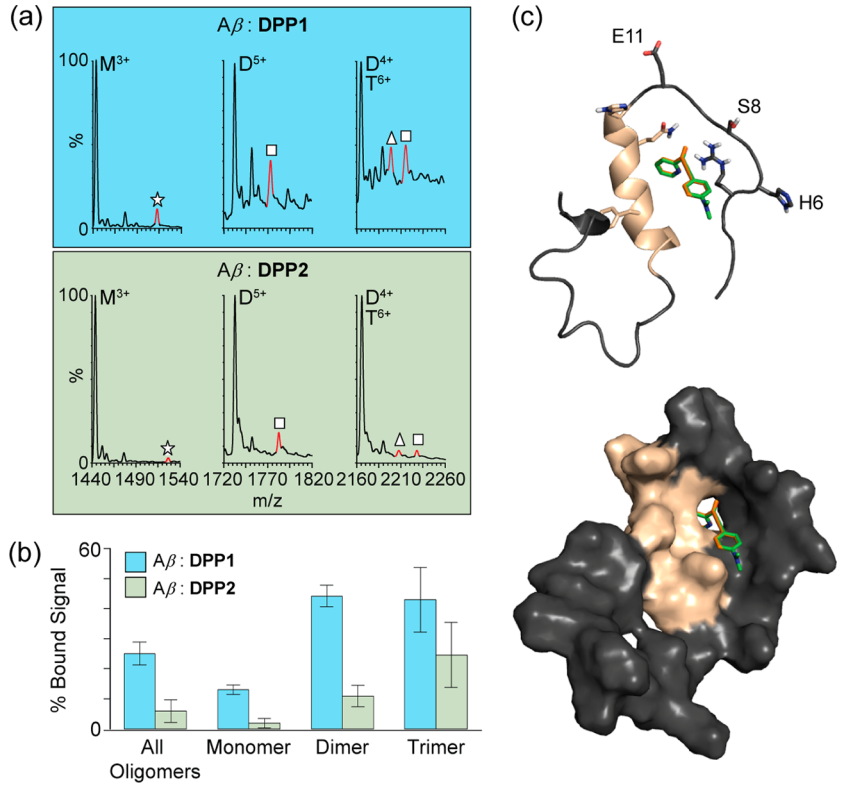

Figure 5. Interactions of **DPP1** and **DPP2** with Aβ. (a) MS data for the complexes of $A\beta_{1-40}$ and **DPP1** or **DPP2** ([Aβ] = 100 μM; [compound] = 600 μM; M = monomer, D = dimer, and T = trimer). Many binding stoichiometries were detected, including 1:1 (star), 2:1 (square), and 3:1 (triangle). (b) A histogram showing the total bound MS signal intensity, normalized for nonspecific interactions and ESI-MS artifacts, for each binding stoichiometry observed in (a). (c) Docking studies of **DPP1** (orange) and **DPP2** (green) with $A\beta_{1-40}$ (PDB 2LFM) by AutoDock Vina. Poses for both compounds were overlapped in this conformation (other conformations, see Figure S4 in the Supporting Information). The helical region of Aβ (H13-D23) is highlighted in color (tan) in both the cartoon (left) and surface (right) representations.

(Figure 5b). Overall, our MS results suggest that although both compounds could interact with Aβ species at high concentrations, **DPP2** was able to bind Aβ species at both low and high concentrations.

To visualize the potential interaction between Aβ and **DPP1**/**DPP2**, docking studies by AutoDock Vina[50] were performed using the previously determined NMR structure (PDB 2LFM)[51] of $A\beta_{1-40}$ monomer. Typically, both compounds were positioned between the α-helix and the unstructured *N*-terminal side of Aβ (Figures 5c and Figure S4 in the Supporting Information). Most docked structures showed a nonspecific orientation of the ligand with respect to the surface features of Aβ. Our preliminary docking studies support the potential interaction of the compounds with Aβ monomer.

Effects of DPP1 and DPP2 on Metal-Free and Metal-Induced Aβ Aggregation in Vitro. Confirming metal binding and Aβ interaction properties (bifunctionality) of **DPP1** and **DPP2**, their influence on in vitro metal-free and metal-induced Aβ aggregation was studied.[26−33] Two different experiments (inhibition and disaggregation) were performed to investigate whether **DPP1**/**DPP2** can control the formation of metal-free and metal-induced Aβ aggregates (inhibition, Figure 6) or transform preformed metal-free and metal-induced Aβ aggregates (disaggregation, see Figure S5 in the Supporting Information). Various-sized Aβ species from both studies were monitored by native gel electrophoresis and SDS-PAGE followed by Western blotting with an anti-Aβ antibody (6E10), whereas morphological changes were identified by transmission electron microscopy (TEM).[26,28−33,53]

The inhibition studies, as shown in Figure 6, demonstrated a different reactivity of **DPP1** or **DPP2** toward metal-induced Aβ species over metal-free Aβ species. In the case of metal-involved Aβ aggregation, Aβ species with a wide range of MW were indicated with **DPP2** for both Cu^{2+}- and Zn^{2+}-treated samples upon longer incubation (Figure 6a, lanes 6 and 9). In the samples containing **DPP1** (lanes 5 and 8), less intense gel bands were detected across the longer incubation time, suggesting that further Aβ aggregation may have occurred. The reaction of **DPP1** or **DPP2** with metal-free Aβ also exhibited a different distribution of various-sized Aβ species (Figure 6a, lanes 2 and 3). Aβ species formed with compounds in both metal-mediated and metal-free conditions were not completely denatured by SDS implying that these molecules may generate different Aβ assemblies (Figure 6b). TEM images of metal-induced Aβ species incubated with **DPP2** for 24 h revealed smaller amorphous aggregates compared to **DPP1**; some of the metal-free Aβ species treated with **DPP1** and **DPP2** presented similar morphology to those untreated with compounds (Figure 6c). Overall, **DPP1** and **DPP2** displayed their ability to recognizably modulate metal-induced Aβ aggregation to different extents.

Furthermore, for the disaggregation experiment (see Figure S5 in the Supporting Information), **DPP2**-treated metal-triggered Aβ aggregates presented different-sized Aβ species than **DPP1**-treated samples, indicating that **DPP2** could alter the properties of preformed Aβ aggregates to a greater extent

dx.doi.org/10.1021/ic302084g | *Inorg. Chem.* 2012, 51, 12959−12967

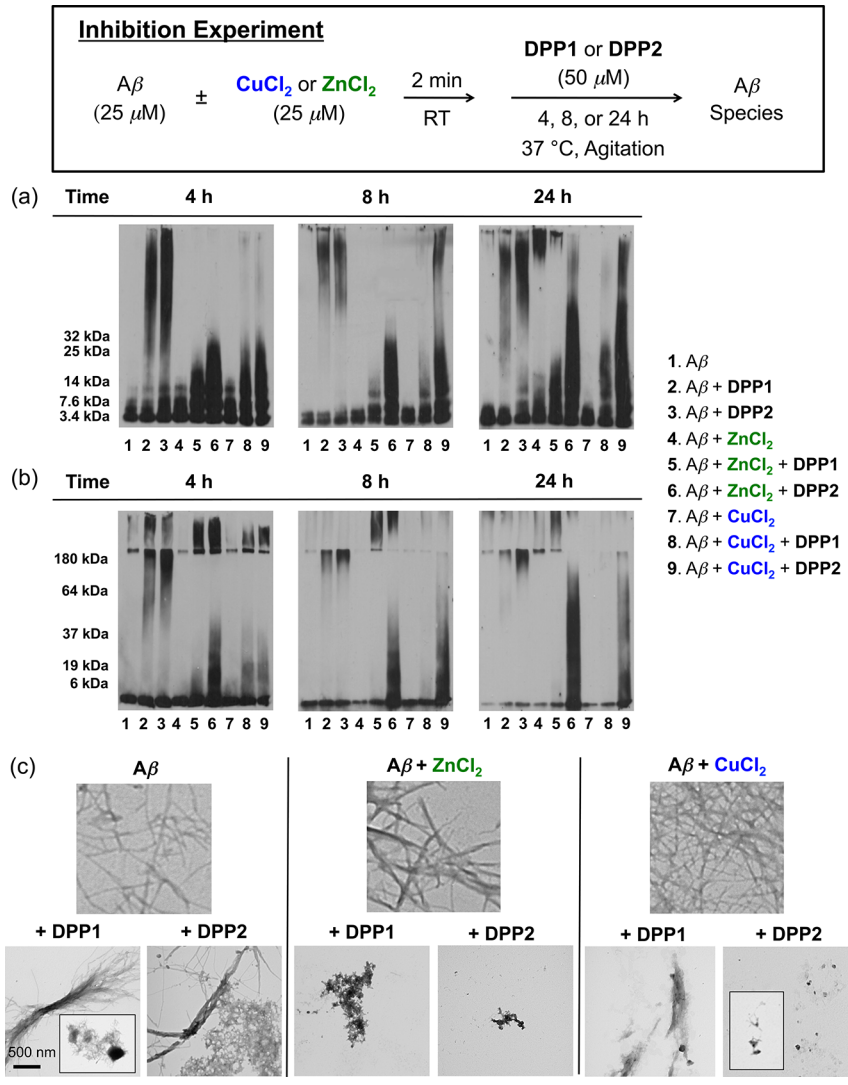

Figure 6. Inhibition experiment (scheme, top). Analysis of various-sized Aβ species by (a) native gel electrophoresis and (b) SDS-PAGE (nonreducing conditions) with Western blot using an anti-Aβ antibody (6E10). (c) TEM images of the 24 h incubated samples. Conditions: [Aβ] = 25 μM; [$CuCl_2$ or $ZnCl_2$] = 25 μM; [compound] = 50 μM; pH 6.6 (for Cu^{2+} samples) or 7.4 (for metal-free and Zn^{2+} samples); 4, 8, or 24 h incubation; 37 °C; constant agitation.

than **DPP1** (see Figure S5a in the Supporting Information). In the metal-free conditions, more various-sized Aβ species were indicated in the presence of **DPP2** than **DPP1** (in particular, at 4 h, Figure S5a, lanes 2 and 3). The Aβ species generated with compounds in both metal-triggered and metal-free conditions were relatively stable in the presence of SDS (see Figure S5b in the Supporting Information). As shown in Figure S5c in the Supporting Information, **DPP2** was able to reorganize preformed structured metal−Aβ aggregates to amorphous species more noticeably than **DPP1**. Taken together, the results from both the inhibition and disaggregation experiments presented that **DPP1** and **DPP2** could regulate metal-involved Aβ aggregation over metal-free aggregation in vitro differently. Moreover, the structural variation (i.e., dimethylamino functionality) may enhance the contact with Aβ species via hydrogen bonding and/or hydrophobic interactions,[29,31,36] which may afford greater reactivity toward metal-Aβ species.

■ SUMMARY AND PERSPECTIVE

Following the incorporation approach, we have developed two bifunctional small molecules (**DPP1** and **DPP2**) composed of a metal chelation site and a diphenylpropynone framework (for Aβ interaction), which could possibly serve as chemical reagents to target and modulate metal−Aβ species in vitro. Their bifunctionality (metal chelation and Aβ interaction) was confirmed by physical methods and preliminary docking studies. Biochemical and TEM studies revealed that **DPP1** and **DPP2** could modulate metal-induced Aβ aggregation in vitro. Notably, **DPP2**, which has a dimethylamino group, exhibited more apparent reactivity toward metal−Aβ species, compared to **DPP1**. This suggests that the interaction and reactivity of molecules with metal−Aβ species can be tuned by such structural variations, proposing a structure-interaction-reactivity relationship. **DPP1** and **DPP2**, however, would be limited in their biological applications since they displayed cytotoxicity in living cells at low micromolar concentrations (see Figure S6 in the Supporting Information). Overall, the promising in vitro reactivity of these potentially BBB-permeable molecules toward metal−Aβ species warrants pursuit of structural modifications that would improve the viability of diphenylpropynone derivatives in biological settings, followed by more detailed characterization by MS and molecular

dx.doi.org/10.1021/ic302084g | Inorg. Chem. 2012, 51, 12959−12967

modeling. Our studies have demonstrated the capability of two diphenylpropynone derivatives to target metal−Aβ species and modulate their interaction and reactivity in vitro, which can be further optimized toward the development of future chemical reagents for investigating metal−Aβ species in biological systems.

■ ASSOCIATED CONTENT

Supporting Information

Table S1 and Figures S1−S6 (PDF). This material is available free of charge via the Internet at http://pubs.acs.org.

■ AUTHOR INFORMATION

Corresponding Author

*E-mail addresses: bruotolo@umich.edu (B.T.R.), mhlim@umich.edu (M.H.L.).

Author Contributions

‡These authors contributed equally.

Notes

The authors declare no competing financial interest.

■ ACKNOWLEDGMENTS

This study was supported by the Alzheimer's Art Quilt Initiative, the Alzheimer's Association (NIRG-10-172326), and the Ruth K. Broad Biomedical Foundation (to M.H.L.), as well as start-up funding from the University of Michigan (to B.T.R.). A.K., M.T.S., and A.S.D. are grateful for the Research Excellence Fellowship from the Department of Chemistry at the University of Michigan, the NIH Training Grant (T32 CA140044), and the NSF Graduate Research fellowship, respectively. We thank Dr. Xiaoming He for synthetic assistance and Nathan Merrill for the NMR measurements for Zn^{2+} binding studies.

■ REFERENCES

(1) Alzheimer's Association. *Alzheimers Dement.* **2012**, *8*, 131−168.
(2) Kepp, K. P. *Chem. Rev.* **2012**, *112*, 5193−5239.
(3) Hardy, J. A.; Higgins, G. A. *Science* **1992**, *256*, 184−185.
(4) Jakob-Roetne, R.; Jacobsen, H. *Angew. Chem., Int. Ed.* **2009**, *48*, 3030−3059.
(5) Rauk, A. *Chem. Soc. Rev.* **2009**, *38*, 2698−2715.
(6) Teplow, D. B.; Lazo, N. D.; Bitan, G.; Bernstein, S.; Wyttenbach, T.; Bowers, M. T.; Baumketner, A.; Shea, J. E.; Urbanc, B.; Cruz, L.; Borreguero, J.; Stanley, H. E. *Acc. Chem. Res.* **2006**, *39*, 635−645.
(7) Scott, L. E.; Orvig, C. *Chem. Rev.* **2009**, *109*, 4885−4910.
(8) DeToma, A. S.; Salamekh, S.; Ramamoorthy, A.; Lim, M. H. *Chem. Soc. Rev.* **2012**, *41*, 608−621.
(9) Haass, C.; Selkoe, D. J. *Nat. Rev. Mol. Cell. Biol.* **2007**, *8*, 101−112.
(10) Lovell, M. A.; Robertson, J. D.; Teesdale, W. J.; Campbell, J. L.; Markesbery, W. R. *J. Neurol. Sci.* **1998**, *158*, 47−52.
(11) Frederickson, C. J.; Koh, J.-Y.; Bush, A. I. *Nat. Rev. Neurosci.* **2005**, *6*, 449−462.
(12) Gaggelli, E.; Kozlowski, H.; Valensin, D.; Valensin, G. *Chem. Rev.* **2006**, *106*, 1995−2044.
(13) Faller, P.; Hureau, C. *Dalton Trans.* **2009**, 1080−1094.
(14) Faller, P. *ChemBioChem* **2009**, *10*, 2837−2845.
(15) Bourassa, M. W.; Miller, L. M. *Metallomics* **2012**, *4*, 721−738.
(16) Zhu, X.; Su, B.; Wang, X.; Smith, M. A.; Perry, G. *Cell. Mol. Life Sci.* **2007**, *64*, 2202−2210.
(17) Zatta, P.; Drago, D.; Bolognin, S.; Sensi, S. L. *Trends Pharmacol. Sci.* **2009**, *30*, 346−355.
(18) Hureau, C.; Faller, P. *Biochimie* **2009**, *91*, 1212−1217.
(19) Bonda, D. J.; Lee, H.-g.; Blair, J. A.; Zhu, X.; Perry, G.; Smith, M. A. *Metallomics* **2011**, *3*, 267−270.
(20) Jomova, K.; Valko, M. *Toxicology* **2011**, *283*, 65−87.
(21) Pithadia, A. S.; Lim, M. H. *Curr. Opin. Chem. Biol.* **2012**, *16*, 67−73.
(22) Hureau, C.; Sasaki, I.; Gras, E.; Faller, P. *ChemBioChem* **2010**, *11*, 950−953.
(23) Braymer, J. J.; DeToma, A. S.; Choi, J.-S.; Ko, K. S.; Lim, M. H. *Int. J. Alzheimers Dis.* **2011**, *2011*, Article ID 623051.
(24) Perez, L. R.; Franz, K. J. *Dalton Trans.* **2010**, *39*, 2177−2187.
(25) Rodríguez-Rodríguez, C.; Telpoukhovskaia, M.; Orvig, C. *Coord. Chem. Rev.* **2012**, *256*, 2308−2332.
(26) Sharma, A. K.; Pavlova, S. T.; Kim, J.; Finkelstein, D.; Hawco, N. J.; Rath, N. P.; Kim, J.; Mirica, L. M. *J. Am. Chem. Soc.* **2012**, *134*, 6625−6636.
(27) Rodríguez-Rodríguez, C.; Sánchez de Groot, N.; Rimola, A.; Álvarez-Larena, Á.; Lloveras, V.; Vidal-Gancedo, J.; Ventura, S.; Vendrell, J.; Sodupe, M.; González-Duarte, P. *J. Am. Chem. Soc.* **2009**, *131*, 1436−1451.
(28) Hindo, S. S.; Mancino, A. M.; Braymer, J. J.; Liu, Y.; Vivekanandan, S.; Ramamoorthy, A.; Lim, M. H. *J. Am. Chem. Soc.* **2009**, *131*, 16663−16665.
(29) Choi, J.-S.; Braymer, J. J.; Nanga, R. P. R.; Ramamoorthy, A.; Lim, M. H. *Proc. Natl. Acad. Sci. U.S.A.* **2010**, *107*, 21990−21995.
(30) Choi, J.-S.; Braymer, J. J.; Park, S. K.; Mustafa, S.; Chae, J.; Lim, M. H. *Metallomics* **2011**, *3*, 284−291.
(31) Braymer, J. J.; Choi, J.-S.; DeToma, A. S.; Wang, C.; Nam, K.; Kampf, J. W.; Ramamoorthy, A.; Lim, M. H. *Inorg. Chem.* **2011**, *50*, 10724−10734.
(32) He, X.; Park, H. M.; Hyung, S.-J.; DeToma, A. S.; Kim, C.; Ruotolo, B. T.; Lim, M. H. *Dalton Trans.* **2012**, *41*, 6558−6566.
(33) Jones, M. R.; Service, E. L.; Thompson, J. R.; Wang, M. C.; Kimsey, I. J.; DeToma, A. S.; Ramamoorthy, A.; Lim, M. H.; Storr, T. *Metallomics* **2012**, *4*, 910−920.
(34) Lipinski, C. A.; Lombardo, F.; Dominy, B. W.; Feeney, P. J. *Adv. Drug Delivery Rev.* **2001**, *46*, 3−26.
(35) Clark, D. E.; Pickett, S. D. *Drug Discovery Today* **2000**, *5*, 49−58.
(36) Leuma Yona, R.; Mazères, S.; Faller, P.; Gras, E. *ChemMedChem* **2008**, *3*, 63−66.
(37) Seregin, I. V.; Schammel, A. W.; Gevorgyan, V. *Org. Lett.* **2007**, *9*, 3433−3436.
(38) Harkat, H.; Blanc, A.; Weibel, J.-M.; Pale, P. *J. Org. Chem.* **2008**, *73*, 1620−1623.
(39) Friel, D. K.; Snapper, M. L.; Hoveyda, A. H. *J. Am. Chem. Soc.* **2008**, *130*, 9942−9951.
(40) Di, L.; Kerns, E. H.; Fan, K.; McConnell, O. J.; Carter, G. T. *Eur. J. Med. Chem.* **2003**, *38*, 223−232.
(41) Avdeef, A.; Bendels, S.; Di, L.; Faller, B.; Kansy, M.; Sugano, K.; Yamauchi, Y. *J. Pharm. Sci.* **2007**, *96*, 2893−2909.
(42) *BBB Protocol and Test Compounds*; pION, Inc.: Woburn, MA, 2009.
(43) Storr, T.; Merkel, M.; Song-Zhao, G. X.; Scott, L. E.; Green, D. E.; Bowen, M. L.; Thompson, K. H.; Patrick, B. O.; Schugar, H. J.; Orvig, C. *J. Am. Chem. Soc.* **2007**, *129*, 7453−7463.
(44) Gans, P.; Sabatini, A.; Vacca, A. *Ann. Chim.* **1999**, *89*, 45−49.
(45) Alderighi, L.; Gans, P.; Ienco, A.; Peters, D.; Sabatini, A.; Vacca, A. *Coord. Chem. Rev.* **1999**, *184*, 311−318.
(46) Braymer, J. J.; Merrill, N. M.; Lim, M. H. *Inorg. Chim. Acta* **2012**, *380*, 261−268.
(47) Reinke, A. A.; Gestwicki, J. E. *Chem. Biol. Drug Des.* **2011**, *77*, 399−411.
(48) Sun, J.; Kitova, E. N.; Wang, W.; Klassen, J. S. *Anal. Chem.* **2006**, *78*, 3010−3018.
(49) Hernández, H.; Robinson, C. V. *Nat. Protocol.* **2007**, *2*, 715−726.
(50) Trott, O.; Olson, A. J. *J. Comput. Chem.* **2010**, *31*, 455−461.
(51) Vivekanandan, S.; Brender, J. R.; Lee, S. Y.; Ramamoorthy, A. *Biochem. Biophys. Res. Commun.* **2011**, *411*, 312−316.
(52) Wolf, L. K. *Chem. Eng. News* **2009**, *87*, 31.
(53) Reinke, A. A.; Seh, H. Y.; Gestwicki, J. E. *Bioorg. Med. Chem. Lett.* **2009**, *19*, 4952−4957.

(54) Ono, M.; Watanabe, H.; Watanabe, R.; Haratake, M.; Nakayama, M.; Saji, H. *Bioorg. Med. Chem. Lett.* **2011**, *21*, 117−120.
(55) Lippard, S. J.; Berg, J. M. *Principles of Bioinorganic Chemistry*; University Science Books: Sausalito, CA, 1994.
(56) Gray, H. B.; Stiefel, E. I.; Valentine, J. S.; Bertini, I. *Biological Inorganic Chemistry: Structure and Reactivity*; University Science Books: Sausalito, CA, 2007.
(57) Bernstein, S. L.; Dupuis, N. F.; Lazo, N. D.; Wyttenbach, T.; Condron, M. M.; Bitan, G.; Teplow, D. B.; Shea, J. E.; Ruotolo, B. T.; Robinson, C. V.; Bowers, M. T. *Nat. Chem.* **2009**, *1*, 326−331.